

ORIGINAL RESEARCH

Hemodynamics in growing and stable cerebral aneurysms

Daniel M Sforza,¹ Kenichi Kono,² Satoshi Tateshima,³ Fernando Viñuela,³ Christopher Putman,⁴ Juan R Cebal¹

¹Center for Computational Fluid Dynamics, College of Sciences, George Mason University, Fairfax, Virginia, USA

²Department of Neurosurgery, Wakayama Rosai Hospital, Wakayama, Japan

³Department of Interventional Neuroradiology, University of California Los Angeles Medical Center, Los Angeles, California, USA

⁴Department of Interventional Neuroradiology, Texas Neurointerventional Surgery Associates, Dallas, Texas, USA

Correspondence to

Dr Daniel M Sforza, Center for Computational Fluid Dynamics, College of Sciences, George Mason University, 4400 University Dr, 101BA Planetary Hall, MSN: 6A2, Fairfax, VA 22030, USA; dsforza@gmu.edu

Received 1 October 2014

Revised 13 January 2015

Accepted 14 January 2015

ABSTRACT

Objective The detailed mechanisms of cerebral aneurysm evolution are poorly understood but are important for objective aneurysm evaluation and improved patient management. The purpose of this study was to identify hemodynamic conditions that may predispose aneurysms to growth.

Methods A total of 33 intracranial unruptured aneurysms longitudinally followed with three-dimensional imaging were studied. Patient-specific computational fluid dynamics models were constructed and used to quantitatively characterize the hemodynamic environments of these aneurysms. Hemodynamic characteristics of growing (n=16) and stable (n=17) aneurysms were compared. Logistic regression statistical models were constructed to test the predictability of aneurysm growth by hemodynamic features.

Results Growing aneurysms had significantly smaller shear rate ratios (p=0.01), higher concentration of wall shear stress (p=0.03), smaller vorticity ratios (p=0.01), and smaller viscous dissipation ratios (p=0.01) than stable aneurysms. They also tended to have larger areas under low wall shear stress (p=0.06) and larger aspect ratios (p=0.18), but these trends were not significant. Mean wall shear stress was not significantly different between growing and stable aneurysms. Logistic regression models based on hemodynamic variables were able to discriminate between growing and stable aneurysms with a high degree of accuracy (94–100%).

Conclusions Growing aneurysms tend to have complex intrasaccular flow patterns that induce non-uniform wall shear stress distributions with areas of concentrated high wall shear stress and large areas of low wall shear stress. Statistical models based on hemodynamic features seem capable of discriminating between growing and stable aneurysms.

INTRODUCTION

Following the International Study of Unruptured Intracranial Aneurysms (ISUIA) study,¹ aneurysm size is the most commonly used factor to assess the risk of rupture and plan the management of patients with intracranial aneurysms. However, it is widely known that small aneurysms do rupture,^{2–3} so other risk factors such as location, gender, and smoking are used to provide some guidance in their evaluation.^{4–5} Of particularly high risk of future rupture are unruptured aneurysms which are enlarging. It is thought that aneurysms develop and progress as a consequence of biologic processes that take place at the wall in response to hemodynamic and biomechanical stimuli which result in the

weakening of the wall, and ultimately rupture when the wall stress exceeds the wall strength.^{5–7} Thus, many researchers have focused on the relationship between hemodynamics and aneurysm growth or rupture. Several investigations have connected a variety of hemodynamic characteristics to aneurysm risk using cross-sectional data.^{8–10} Others have used longitudinal data to study the hemodynamic conditions in growing aneurysms^{11–12} and to compare hemodynamic characteristics between stable aneurysms and aneurysms that ruptured during observation.^{13–14} However, the exact mechanisms that drive the aneurysms towards rupture remain poorly understood, preventing a precise risk assessment.¹⁵ Since previous studies have associated aneurysm growth with rupture,^{16–17} the purpose of our study was to identify hemodynamic conditions that may predispose aneurysms to growth and rupture using longitudinal data of untreated intracranial aneurysms.

METHODS

The hemodynamic characteristics of a series of growing and stable unruptured aneurysms followed without treatment were derived from image-based computational models and compared. The methodology is schematically summarized in [figure 1](#) and described in more detail below.

Clinical data

A total of 33 untreated intracranial aneurysms longitudinally followed with three-dimensional (3D) imaging were identified in 21 patients and selected for study from our database. The criteria for inclusion in the study were untreated aneurysms with at least two 3D images spaced over a period of at least 9 months. 3D CT angiography or rotational angiography images were collected from the initial examination and from later follow-up observations. Expert neuroradiologists initially screened growing aneurysms by size measurements using the standard clinical approach of measuring the maximum diameter on a 2D image slice-plane. This standard procedure makes comparisons of measurements on images at different times difficult because it does not guarantee measurements in the same slice-plane or direction. This problem is usually not addressed in research papers. To overcome this difficulty, we developed a method to objectively measure aneurysm geometrical changes over a period of time. After segmentation and geometry reconstruction, vascular models corresponding to different times were aligned and the distance map was calculated.

To cite: Sforza DM, Kono K, Tateshima S, et al. *J NeuroIntervent Surg* Published Online First: [please include Day Month Year] doi:10.1136/neurintsurg-2014-011339

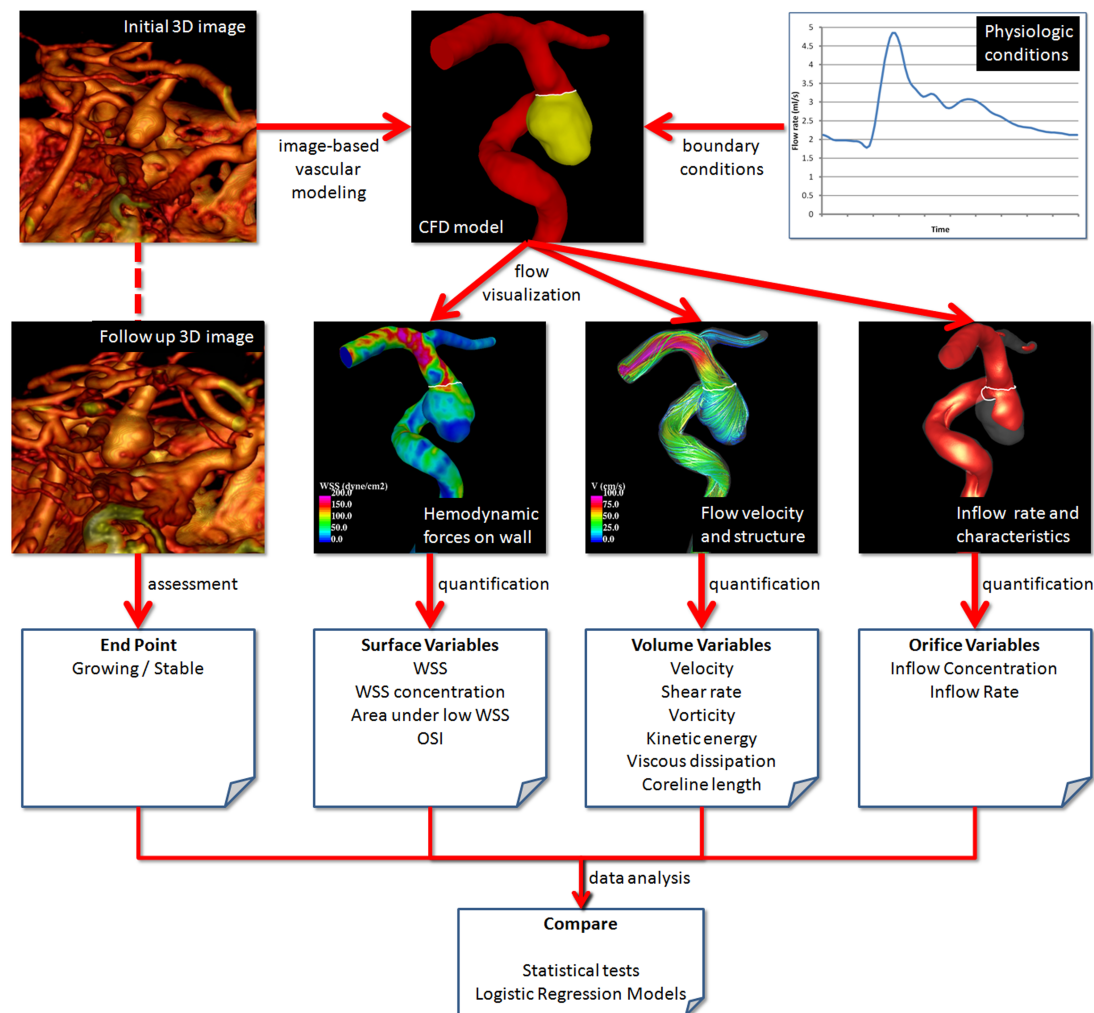


Figure 1 Methodology overview: image-based computational modeling of longitudinally followed untreated aneurysms, visualization and quantification of hemodynamic characteristics and statistical data analysis. OSI, oscillatory shear index; WSS, wall shear stress.

The alignment was done by removing the aneurysms at the neck and aligning the parent vessels by minimizing the distance between the models. Aneurysms exhibiting an increase in size (displacement) of >0.5 mm in any direction on at least 5% of the aneurysm points from the initial examination were classified as ‘growing’; aneurysms that did not enlarge >0.5 mm for at least 9 months were classified as ‘stable’. The 0.5 mm threshold was chosen to be larger than the average voxel resolution (a measure of the precision on the geometry determination). A total of 16 aneurysms were included in our study as growing and 17 aneurysms as stable. The patients’ ages ranged from 42 to 81 years (mean (SD) 67 (13) years). Fourteen aneurysms were located in the internal carotid artery (ICA), seven in the posterior communicating artery, six in the anterior communicating artery, five in the middle cerebral artery (MCA), and one in the basilar artery (BA). Aneurysm sizes ranged from 2.41 to 20.9 mm (mean (SD) 7.25 (4.52) mm). There was no statistical difference between the size of growing and stable aneurysms.

Aneurysm modeling

Patient-specific vascular models were constructed from the 3D images of the initial examination. Segmentation was carried out using region growing and deformable models.¹⁸ Models were smoothed and truncated perpendicularly to the vessel axis, keeping as much of the proximal parent artery as possible to

ensure proper representation of secondary swirling flows in the parent artery and aneurysm orifice.¹⁹ Unstructured grids were generated with a resolution of 0.2 mm. Blood was approximated as a Newtonian fluid with density $\rho=1.0$ g/cm³ and viscosity $\mu=0.04$ Poise. The incompressible Navier–Stokes equations were numerically solved using in-house finite elements solver.²⁰ Pulsatile low boundary conditions were imposed at the model inlet using the Womersley profile.²¹ The flow waveform was derived from phase-contrast MR measurements in the ICA and vertebral artery of normal subjects²² and scaled with the inlet boundary area.²³ All inlet boundaries were located in the ICA, except for one case where the aneurysm was located in the BA and the two inlets were located in the vertebral arteries. The flow from the parent artery was split among the outlet boundaries according to the principle of minimum work (Murray’s law).²⁴ Wall compliance was neglected and no-slip boundary conditions were applied at the walls. Numerical simulations were carried out for two cardiac cycles and the flow field was saved at 0.01 s intervals during the second cycle for subsequent analysis.

Hemodynamics characterization

Aneurysm necks were delineated on the reconstructed models. A few points on the neck were interactively selected and connected along lines of minimum geodesic distance. Next, the aneurysm orifice was triangulated and used to subdivide the

computational mesh into two regions corresponding to the aneurysm and the parent artery. A number of flow variables defined on the aneurysm surface, volume, or orifice were quantified and used to characterize the aneurysm hemodynamics. Volumetric factors included: kinetic energy ratio (KER), which measures the mean kinetic energy in the aneurysm with respect to the mean kinetic energy in the parent artery; velocity ratio (VER), which measures the mean aneurysm velocity with respect to the mean parent artery velocity; shear rate ratio (SRR), defined as the mean aneurysm shear rate (a measure of the deformation of the fluid elements) divided by the mean shear rate of the parent artery; vorticity ratio (VOR), defined as the ratio of the mean aneurysm vorticity (a measure of the rotational velocity of fluid elements) over the mean artery vorticity; viscous dissipation ratio (VDR), which measures the amount of viscous energy dissipation in the aneurysm with respect to that in the parent artery; and vortex coreline length (CORELEN), which provides a measure of the complexity of the aneurysmal flow structure.²⁵ Surface factors included mean, maximum and minimum wall shear stress (WSS, WSSMAX, WSSMIN) computed over the aneurysm sac; shear concentration index (SCI), which measures the degree of concentration of the WSS distribution; percentage of the aneurysm area under low WSS (LSA), where low WSS is defined as 1 SD below the mean WSS in the parent artery; and mean oscillatory shear index (OSI). Hemodynamic factors defined over the aneurysm orifice included mean inflow rate and inflow concentration index (ICI), which measures the degree of concentration of the inflow stream. Additionally, a number of geometric variables were calculated including aneurysm size (maximum distance between two points on the dome); aneurysm depth (maximum distance from the aneurysm dome to the orifice); maximum neck size; aneurysm area; neck area; and aspect ratio. More details and exact definitions of these variables are provided by Mut *et al.*²⁶

Data analysis

Mean values of hemodynamics and geometric variables over the growing and stable aneurysm groups were calculated and compared. Non-parametric Wilcoxon rank sum tests were performed to determine the statistical significance of the differences between growing and stable aneurysms. Differences were considered statistically significant if the *p* values were <0.05 (95% confidence).

Predictive statistical models based on hemodynamic variables were then created and tested. Logistic regression models²⁷ were trained with data from all except one aneurysm and then tested on the aneurysm that was left out. The process was repeated by leaving each aneurysm out in turn, and the accuracy of the predictive model was calculated by counting the number of aneurysm states (growing or stable) that were correctly predicted. The accuracies of models based on different sets of hemodynamic variables (features) were compared.

RESULTS

Aneurysm characteristics and geometry are presented in [table 1](#). The mean and SD of each hemodynamic factor computed over the growing and stable aneurysm groups are listed in [table 2](#). Statistically significant differences were obtained for SRR, VOR, VDR, and SCI while marginal statistical significance (*p*<0.06) was obtained for LSA.

The ratios of the mean values of the growing aneurysm group over the stable aneurysm group are plotted in [figure 2](#) (blue bars). Ratios of the mean values of ruptured over unruptured aneurysms from a previous study²⁸ are also included for

comparison (red bars). In this graph, bars above or below 1 indicate that the mean value of the corresponding hemodynamic variable is on average larger or smaller in growing (ruptured) than in stable (unruptured) aneurysms, and by how much. Statistically significant differences are indicated by a solid outline while marginal significance is indicated with a dashed outline. Bars without an outline correspond to variables that are not statistically different between the aneurysm groups.

Logistic regression models were constructed for each hemodynamic variable in turn and the corresponding accuracy was calculated using the leave-one-out method described previously. New logistic regression models were then constructed by combining pairs of the hemodynamic variables that gave the best accuracy in single-variable models. Models based on the vortex CORELEN and the ICI were able to successfully discriminate all growing and stable aneurysms (100% accuracy). The next best discriminators were the OSI with 97% accuracy, the area under low WSS (LSA) and the minimum WSS, both with an accuracy of 94%. Models based on two variables that yielded a better accuracy than these single-feature models (except for the one based on CORELEN or ICI) included high inflow concentration and high OSI, and large area under low WSS and high OSI, both with an accuracy of 100%.

DISCUSSION

The few previous studies that analyzed the hemodynamics in growing intracranial aneurysms using longitudinal data have had mixed results. One study analyzed the hemodynamics in growing aneurysms (*n*=7) and suggested that growth occurs at regions of abnormally low WSS.¹¹ Another study analyzed the hemodynamics in a pair of tandem aneurysms (*n*=2) of the posterior inferior cerebellar artery and showed that one had high flow and high WSS in the region of growth while the other had low flow and low WSS.¹² Thus, they concluded that the growing region could be either near the inflow zone and exposed to high WSS or in the aneurysm sac and exposed to low WSS and high OSI. Similarly, two other studies that analyzed the hemodynamics in aneurysms that ruptured during observation did not find consistency in the association of hemodynamic variables with rupture. The first compared 26 stable aneurysms and six aneurysms that ruptured during observation and found that the aneurysms that ruptured had larger 'energy loss' but the mean WSS was similar between the two groups.¹³ The second study analyzed 50 ICA aneurysms (6 ruptured, 44 stable) and 50 MCA aneurysms (7 ruptured, 43 stable) and found that the 'pressure loss' coefficient was smaller in ruptured aneurysms at both locations, minimum WSS was lower in ruptured ICA aneurysms but not in ruptured MCA aneurysms, and mean WSS, maximum WSS, OSI and 'energy loss' were not different between ruptured and stable aneurysms.¹⁴

Most previous studies have focused on measures of wall/flow interactions, primarily WSS, following the hypothesis that WSS is the principal signal to the endothelial cells which are linked to wall remodeling. The finding that 'energy loss' rather than WSS measures correlated to rupture in the study by Qian *et al.*¹³ raises the interesting possibility that hemodynamics occurring within the volume of the aneurysm sac may be used as a predictor instead of WSS. In an early study of a population of both ruptured and unruptured aneurysms using a number of qualitative assessments of intra-aneurysmal flow patterns, Czebrat *et al.*²⁹ found that 'complex and unstable' flow patterns were associated with aneurysms that had previously ruptured. Our study chose hemodynamic quantities to compare growing (*n*=16) and stable (*n*=17) unruptured aneurysms, which

Table 1 Patient and aneurysm characteristics

No	Location	Size (mm)	Area (mm ²)	Volume (mm ³)	Aspect ratio	Follow-up (months)	Size difference		Area difference		Volume difference		Aspect ratio difference (%)	Max Disp (mm)	Status
							mm	%	mm ²	%	mm ³	%			
1	L PCOM	10.2	200.6	1688.4	1.14	30	1.71	16.8	53.4	26.6	692.4	41	13.7	1.598	Growing
2	ACOM	10.1	180.4	1427.9	1.18	14	0.9	8.9	16.8	9.3	150.9	10.6	14.3	0.779	
3	R Cavernous ICA	4.5	28.3	92	0.6	35	0.5	11.1	3.8	13.3	18.9	20.6	-21.5	0.96	
4	ACOM	6.7	66.7	329.4	0.71	27	1.03	15.5	20.1	30.1	160.6	48.8	5.5	0.862	
5	R Cavernous CA	7.9	82.3	442.2	0.5	25	-0.78	-9.8	-13.1	-16	794.3	179.6	-4	1.366	
6	L MCA bifurcation	20.9	762.2	10 950.1	5.12	58	0.75	3.6	23.8	3.1	949.2	8.7	6.7	0.978	
7	BA trunk	19.5	586.5	8608.2	0.64	31	3.41	17.4	267.5	45.6	7152.6	83.1	11.2	3.52	
8	R Cavernous ICA	10.7	192	1594.3	0.79	73	0.15	1.4	3.5	1.8	36	2.3	-12.2	0.968	
9	L ICA terminus	4.4	18.2	35.8	0.69	25	0.49	11.3	8.7	47.7	34.2	95.5	-5.2	0.633	
10	L PCOM	2.9	9.8	2.9	0.43	49	0.63	22.2	9.1	92.7	5.3	180	48.7	0.849	
11	L PCOM	2.5	5.5	0.8	0.17	49	0.2	8.2	1.6	29.8	1.2	164.3	121	0.558	
12	L PCOM	11.9	328.7	605.3	1.12	72	5.6	47	359.8	109.4	1142.7	188.8	13.9	4.708	
13	L PCOM	3.7	22.2	10.8	0.69	38	1.25	33.6	18.8	85	15.2	141	7.3	1.276	
14	L PCOM	5.1	46.7	31.9	0.65	30	3.62	71	51.2	109.8	39.4	123.5	117	0.989	
15	ACOM	3.9	24.9	71.8	0.89	13	0.67	17.2	9.7	39.1	44.1	61.5	40.8	0.568	
16	ACOM	5.4	45.1	174.5	0.7	5	0.43	8	4.5	10	13.3	7.6	31	0.772	
17	ACOM	9.8	193.4	1679.5	0.86	28	-0.46	-4.7	-5.5	-2.9	-88.9	-5.3	8	0.424	
18	R MCA bifurcation	8.3	142.8	1087.9	0.93	23	0.24	2.9	6.7	4.7	60.1	5.5	-0.3	0.343	
19	R ICA s. Hyp.	9.5	187.5	1486.8	1.22	35	-0.33	-3.5	-4	-2.2	-43.4	-2.9	1.6	0.669	
20	L ICA s. Hyp.	12.1	251.5	2254.5	1.21	37	0.79	6.5	6.3	2.5	32	1.4	13	0.485	
21	L ICA supracl.	4.2	19.5	85	0.38	37	0.02	0.5	2.9	14.7	-22.5	-26.5	7.9	0.485	
22	R PCOM	5.4	32.6	98.6	0.39	25	-0.13	-2.4	-2.7	-8.2	-16.2	-16.5	19.8	0.175	
23	R MCA bifurcation	8.3	137.3	956.5	1.05	25	-0.54	-6.5	-18.2	-13.2	-199	-20.8	-3	0.496	
24	R ICA s. Hyp.	4.5	23.8	57.6	0.43	15	0.05	1.2	-0.1	-0.3	2.9	5.1	-4.4	0.301	
25	R ICA terminus	2.8	9.5	15.8	0.36	15	0.17	6.3	0.1	0.6	-0.2	-1.3	-5.7	0.303	
26	R MCA bifurcation	3.7	18.7	46.9	0.66	15	0.06	1.5	1.9	10.4	11.9	25.4	7.3	0.214	
27	R M2 bifurcation	2.9	8.7	15.4	0.33	15	-0.07	-2.4	-0.2	-2.8	-0.5	-3	2.1	0.264	
28	L ICA i. Hyp.	4.3	27.5	70.3	0.47	10	0.2	4.5	0.1	0.5	6.8	9.6	12.8	0.199	
29	L ICA s. Hyp	2.9	7	8.2	0.25	10	0.37	12.5	2.1	30.2	5	60.9	-2.8	0.283	
30	L ICA oph.	2.4	7	9.4	0.36	10	0.05	2	0.2	3.1	0.4	4.6	9.4	0.281	
31	L ICA oph.	5.5	55.1	233.9	1.12	10	0.21	3.9	2.1	3.8	14	6	5.5	0.287	
32	R ICA oph.	4.6	20.2	46.2	0.33	73	0.9	19.6	7.3	36.2	28.7	62.2	-12	0.426	
33	ACOM	6.4	55.6	161.9	0.31	9	0.31	4.8	0.2	0.4	40	24.7	21.9	0.493	

ACOM, anterior communicating artery; BA, basilar artery; i. Hyp, inferior Hypophysial; ICA, internal carotid artery; max disp, maximum displacement; MCA, middle cerebral artery; oph, ophthalmic; PCOM, posterior communicating artery; s. Hyp, superior Hypophysial; Supracl, supraclinoid.

Table 2 Statistics of hemodynamic variables

Variable	Growing group		Stable group		p Value
	Mean	SD	Mean	SD	
ICI	0.87	0.81	0.60	0.64	0.12
KER	0.29	0.23	0.63	1.14	0.19
SRR	0.74	0.50	1.17	0.55	0.01*
VER	0.49	0.23	0.64	0.45	0.20
VOR	0.71	0.42	1.13	0.49	0.01*
VDR	0.72	1.01	1.80	1.58	0.01*
WSSMAX (dyne/cm ²)	338.37	200.60	298.79	125.48	0.34
WSSMIN (dyne/cm ²)	2.71	7.85	2.21	3.79	0.38
WSS (dyne/cm ²)	37.78	30.25	41.98	22.73	0.22
SCI	4.16	2.81	2.59	1.25	0.03*
LSA (%)	40.58	29.58	24.17	22.83	0.06
OSI	0.01	0.02	0.01	0.01	0.35
CORELEN	2.49	4.42	0.87	0.88	0.11

*Statistically significant differences (95% confidence).

CORELEN, coreline length; ICI, inflow concentration index; KER, kinetic energy ratio; LSA, aneurysm area under low WSS; OSI, oscillatory shear index; SCI, shear concentration index; SRR, shear rate ratio; VDR, viscous dissipation ratio; VER, velocity ratio; VOR, vorticity ratio; WSS, wall shear stress; WSSMAX, maximum wall shear stress; WSSMIN, minimum wall shear stress.

separated the hemodynamic characteristics into three basic compartments: entry events (ICI), intrasaccular flow characteristics (KER, SRR, VER, VOR, VDR, CORELEN), and wall/flow interactions (WSSMax, WSSMin, SCI, LSA, OSI), in an effort to separate the hemodynamic events more systematically. Furthermore the intrasaccular measures were chosen to find objective measures that could further define the characteristics of complex flow patterns. Increased SRR, VER, VOR, and VDR indicate a greater interaction between the intrasaccular flow streams leading to a dissipation of the forces from fluid to fluid interactions. CORELEN is increased in situations with multiple vortices, as in the qualitative complex flow patterns described by Byrne *et al.*²⁵

Our study found statistical associations between increased SCI, low SRR, VDR and VOR, and a trend toward elevated LSA. Thus, growing aneurysms had on average more concentrated WSS, lower viscous dissipation than their parent artery, and

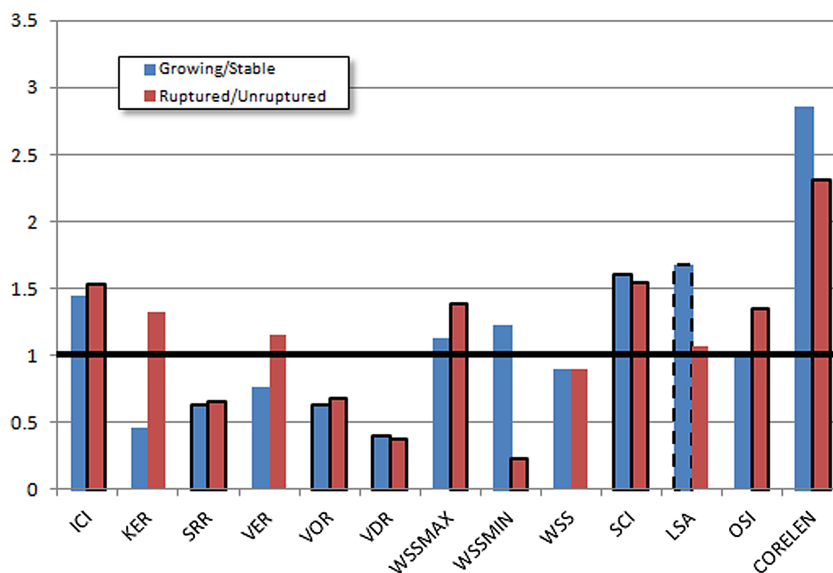
lower local deformation and rotation of fluid elements than their parent artery. Although not statistically significant, CORELEN trended to be larger on growing aneurysms. The mean WSS was not significantly different between growing and stable aneurysms. These results seem to suggest that concentrated inflow streams that spread into complex intrasaccular flow patterns that induce non-uniform WSS distributions with areas of concentrated high WSS and large areas of low WSS could represent the characteristics of hemodynamic environments that predispose aneurysms to growth. The same trends were observed when comparing ruptured and unruptured aneurysms from a previous cross-sectional aneurysm series (figure 2).²⁸

However, several notable differences between the two groups are found in the measures of fluid to wall interactions. Ruptured aneurysms had larger maximum WSS and larger OSI, trends that were not observed in our series of growing versus stable aneurysms. The area of the aneurysm under low WSS was found to be larger in growing aneurysms than in stable aneurysms but it was found to be similar between ruptured and unruptured aneurysms. Finally, the minimum WSS was found to be lower in ruptured aneurysms than in unruptured aneurysms but larger in growing aneurysms than in stable aneurysms. These differences need to be confirmed in larger datasets, but suggest the possibility of more than one mechanism in play.

Our statistical analysis using logistic regression models suggests that hemodynamic conditions can be used to identify aneurysms that are likely to grow or rupture. However, to establish a general predictive model, larger studies involving multiple populations are required with consideration of other risk factors.

Assessing geometrical changes during aneurysm evolution is challenging. Usually this is simply done by measuring size on a slice-plane. However, this approach may be unreliable—for example, one aneurysm in our sample (see table 1) almost doubled its volume but reduced its diameter (ie, by changing from an ellipsoid to a more spherical shape). It is also possible to maintain the volume (or size) but have a substantial change in shape. Hence, we quantified shape changes by calculating the distances between aneurysm surfaces at different times after alignment of the parent arteries. We believe that a 3D measurement of geometrical changes is more reliable than the usual method. In fact, some aneurysms initially classified as ‘growing’

Figure 2 Ratio of hemodynamic variables averaged over growing and stable aneurysms (blue bars) compared with ruptured and unruptured aneurysms (red bars). Statistically significant differences are indicated by solid contours and marginally significant differences are indicated by dashed contours. CORELEN, coreline length; ICI, inflow concentration index; KER, kinetic energy ratio; LSA, aneurysm area under low WSS; OSI, oscillatory shear index; SCI, shear concentration index; SRR, shear rate ratio; VDR, viscous dissipation ratio; VER, velocity ratio; VOR, vorticity ratio; WSS, wall shear stress; WSSMAX, maximum wall shear stress; WSSMIN, minimum wall shear stress.



by the usual method were classified as 'stable' by the 3D method.

Our study has a number of limitations. Aneurysms included in the study suffered from a selection bias because aneurysms typically selected for conservative observation are already considered relatively safe. Our study is not a case-control study with matching growing and stable aneurysms. The classification of aneurysms into growing or stable groups is not unique; it depends on the follow-up time and the speed of progression. We considered an aneurysm stable if geometrical changes were smaller than 0.5 mm over a period of at least 9 months, consistent with clinical practice. If larger changes were observed, the aneurysms were classified as growing. However, it is not possible to know whether stable aneurysms are truly stable or if they are growing very slowly. Similarly, with our current data it is not possible to determine whether or not growing aneurysms are slowing down and eventually stabilizing. More precise determination of the progression status of the aneurysms would require longer follow-up periods and probably more frequent imaging. Under these considerations one could refer to our 'growing' group as 'fast changing' and to our 'stable' group as 'slowly changing'. The average follow-up times for growing and stable group were 36 and 23 months, respectively. Although these times were not equal, the assumptions previously discussed still allow a meaningful comparison. The relatively small sample size did not allow us to study the possible effects of aneurysm location. Growing and stable unruptured aneurysms were selected from a database of untreated patients when longitudinal imaging studies were available. Finally, computational fluid dynamics models make several assumptions such as rigid walls, Newtonian flows, normal physiologic conditions, etc (for a new approach to boundary conditions see McGah *et al*³⁰). Despite these limitations, interesting observations could be made—namely, that growing and stable aneurysms share some associations with ruptured and unruptured aneurysms but also present interesting differences that should be taken into consideration when investigating the mechanisms responsible for aneurysm progression and rupture.

CONCLUSIONS

Compared with stable aneurysms, growing aneurysms tend to have complex intrasaccular flow patterns that induce non-uniform WSS distributions with areas of concentrated high WSS and large areas of low WSS. Statistical models based on hemodynamic features seem capable of discriminating between growing and stable aneurysms.

Moreover, assessing geometrical changes by measuring size on a slice-plane may be unreliable. The 3D method is potentially a better method which, although difficult to implement at a clinical level at present, could have a place in the near future if an automated protocol is implemented in medical imaging equipment.

Contributors DMS: study design, data preparation, analysis and interpretation, manuscript preparation including tables and draft of final manuscript version. KK: data collection and interpretation, critical revision of manuscript. ST: data collection and critical revision of manuscript. FV and CP: data collection, study design, critical revision of manuscript. JRC: study design, data interpretation and analysis, manuscript and figure preparation, critical revision of manuscript.

Funding This work was supported by the National Institutes of Health grant numbers R01 NS59063 and R21 NS075341.

Competing interests None.

Ethics approval Ethics approval was obtained from the Office of Research Integrity and Assurance, George Mason University.

Provenance and peer review Not commissioned; externally peer reviewed.

Data sharing statement Models and simulation data are available upon request.

REFERENCES

- Wiebers DO, Whisnant JP, Huston J III, *et al*. Unruptured intracranial aneurysms: natural history, clinical outcome, and risks of surgical and endovascular treatment. *Lancet* 2003;362:103–10.
- Beck J, Rohde S, Berkefeld J, *et al*. Size and location of ruptured and unruptured intracranial aneurysms measured by 3-dimensional rotational angiography. *Surg Neurol* 2006;65:18–25.
- Joo SW, Lee SI, Noh SJ, *et al*. What is the significance of a large number of ruptured aneurysms smaller than 7 mm in diameter? *J Korean Neurosurg Soc* 2009;45:85–9.
- Seibert B, Tummala RP, Chow R, *et al*. Intracranial aneurysms: review of current treatment options and outcomes. *Front Neurol* 2011;2:45.
- Cebral JR, Raschi M. Suggested connections between risk factors of intracranial aneurysms: a review. *Ann Biomed Eng* 2013;41:1366–83.
- Sadasivan C, Fiorella DJ, Woo HH, *et al*. Physical factors effecting cerebral aneurysm pathophysiology. *Ann Biomed Eng* 2013;41:1347–65.
- Isaksen JG, Bazilevs Y, Kvamsdal T, *et al*. Determination of wall tension in cerebral artery aneurysms by numerical simulation. *Stroke* 2008;39:3172–8.
- Shojima M, Oshima M, Takagi K, *et al*. Role of the bloodstream impacting force and the local pressure elevation in the rupture of cerebral aneurysms. *Stroke* 2005;36:1933–8.
- Cebral JR, Castro MA, Burgess JE, *et al*. Characterization of cerebral aneurysm for assessing risk of rupture using patient-specific computational hemodynamics models. *AJNR Am J Neuroradiol* 2005;26:2550–9.
- Xiang J, Natarajan SK, Tremmel M, *et al*. Hemodynamic-morphologic discriminants for intracranial aneurysm rupture. *Stroke* 2011;42:144–52.
- Boussel L, Rayz V, McCulloch C, *et al*. Aneurysm growth occurs at region of low wall shear stress: patient-specific correlation of hemodynamics and growth in a longitudinal study. *Stroke* 2008;39:2997–3002.
- Sugiyama SI, Meng H, Funamoto K, *et al*. Hemodynamic analysis of growing intracranial aneurysms arising from a posterior inferior cerebellar artery. *World Neurosurg* 2012;78:462–8.
- Qian Y, Takao H, Umezumi M, *et al*. Risk analysis of unruptured aneurysms using computed fluid dynamics technology: preliminary results. *AJNR Am J Neuroradiol* 2011;32:1948–55.
- Takao H, Murayama Y, Ishibashi Y. Hemodynamic differences between unruptured and ruptured intracranial aneurysms during observation. *Stroke* 2012;43:1436–9.
- Sforza D, Putman CM, Cebral JR. Hemodynamics of cerebral aneurysms. *Ann Rev Fluid Mechanics* 2009;41:91–107.
- Chmaysani M, Rebeiz JG, Rebeiz TJ, *et al*. Relationship of growth to aneurysm rupture in asymptomatic aneurysms ≤ 7 mm: a systematic analysis of the literature. *Neurosurgery* 2011;68:1164–71.
- Juvela S, Poussa K, Porras M. Factors affecting formation and growth of intracranial aneurysms: a long-term follow-up study. *Stroke* 2001;32:485–91.
- Cebral JR, Castro MA, Appanaboyina S, *et al*. Efficient pipeline for image-based patient-specific analysis of cerebral aneurysm hemodynamics: technique and sensitivity. *IEEE Trans Med Imag* 2005;24:457–67.
- Castro MA, Putman CM, Cebral JR. Computational fluid dynamics modeling of intracranial aneurysms: effects of parent artery segmentation on intra-aneurysmal hemodynamics. *AJNR Am J Neuroradiol* 2006;27:1703–9.
- Löhner R. *Applied CFD techniques*. John Wiley & Sons, 2001.
- Taylor CA, Hughes TJR, Zangl CK. Finite element modeling of blood flow in arteries. *Comp Meth App Mech Eng* 1998;158:155–96.
- Ford MD, Alperin N, Lee SH, *et al*. Characterization of volumetric flow rate waveforms in the normal internal carotid and vertebral arteries. *Physiol Meas* 2005;26:477–88.
- Cebral JR, Castro MA, Putman CM, *et al*. Flow-area relationship in internal carotid and vertebral arteries. *Physiol Meas* 2008;29:585–94.
- Murray CD. The physiological principle of minimum work applied to the angle of branching of arteries. *J Gen Physiol* 1926;9:835–41.
- Byrne G, Mut F, Cebral JR. Quantifying the large-scale hemodynamics of intracranial aneurysms. *AJNR Am J Neuroradiol* 2014;35:333–8.
- Mut F, Löhner R, Chien A, *et al*. Computational hemodynamics framework for the analysis of cerebral aneurysms. *Int J Num Meth Biomed Eng* 2011;27:822–39.
- Fan RE, Chang KW, Hsieh CJ, *et al*. LIBLINEAR: a library for large linear classification. *J Mach Learn Res* 2008;9:1871–4.
- Cebral JR, Mut F, Weir J, *et al*. Quantitative characterization of the hemodynamic environment in ruptured and unruptured brain aneurysms. *AJNR Am J Neuroradiol* 2011;32:145–51.
- Cebral JR, Mut F, Weir J, *et al*. Association of hemodynamic characteristics and cerebral aneurysm rupture. *AJNR Am J Neuroradiol* 2011;32:264–70.
- McGah PM, Levitt MR, Barbour MC, *et al*. Accuracy of computational cerebral aneurysm hemodynamics using patient-specific endovascular measurements. *Ann Biomed Eng* 2014;42:503–14.



Hemodynamics in growing and stable cerebral aneurysms

Daniel M Sforza, Kenichi Kono, Satoshi Tateshima, Fernando Viñuela, Christopher Putman and Juan R Cebral

J NeuroIntervent Surg published online February 4, 2015

Updated information and services can be found at:

<http://jnis.bmj.com/content/early/2015/02/04/neurintsurg-2014-011339>

References

These include:

This article cites 29 articles, 13 of which you can access for free at: <http://jnis.bmj.com/content/early/2015/02/04/neurintsurg-2014-011339#BIBL>

Email alerting service

Receive free email alerts when new articles cite this article. Sign up in the box at the top right corner of the online article.

Topic Collections

Articles on similar topics can be found in the following collections

[Basic science](#) (80)

Notes

To request permissions go to:

<http://group.bmj.com/group/rights-licensing/permissions>

To order reprints go to:

<http://journals.bmj.com/cgi/reprintform>

To subscribe to BMJ go to:

<http://group.bmj.com/subscribe/>